Stem Cell Research 29 (2018) 245–249

Contents lists available at ScienceDirect

Stem Cell Research

journal homepage: www.elsevier.com/locate/scr

Lab Resource: Multiple Cell Lines

Generation of an induced pluripotent stem cell line from a patient with non-syndromic *CLN3*-associated retinal degeneration and a coisogenic control line

Xiao Zhang[a,b], Dan Zhang[a,b], Shang-Chih Chen[a,b], Tina Lamey[a,c], Jennifer A. Thompson[c], Terri McLaren[c], John N. De Roach[a,c], Fred K. Chen[a,b,c,d,*], Samuel McLenachan[a,b]

[a] *Centre for Ophthalmology and Visual Science, The University of Western Australia, Perth, Western Australia, Australia*
[b] *Lions Eye Institute, Nedlands, Western Australia, Australia*
[c] *Australian Inherited Retinal Disease Registry and DNA Bank, Department of Medical Technology and Physics, Sir Charles Gairdner Hospital, Perth, Western Australia, Australia*
[d] *Royal Perth Hospital, Perth, Western Australia, Australia*

A B S T R A C T

We report the generation of the human iPSC line LEIi004-A from a patient with late-onset non-syndromic retinitis pigmentosa caused by compound heterozygous mutations in the *CLN3* gene. Reprogramming of primary dermal fibroblasts was performed using episomal plasmids containing *OCT4*, *SOX2*, *KLF4*, *L-MYC*, *LIN28*, shRNA for *p53* and mir302/367 microRNA. To create a coisogenic control line, one *CLN3* variant was corrected in the patient-iPSC using CRISPR/Cas9 gene editing to generate the iPSC line LEIi004-A-1.

Resource table.

Unique stem cell lines identifier	LEIi004-A LEIi004-A-1
Alternative names of stem cell lines	NO
Institution	The University of Western Australia
Contact information of distributor	Dr Fred K Chen fredchen@uwa.edu.au
Type of cell lines	iPSC
Origin	Human, 52 year old caucasian female
Cell Source	Fibroblasts
Clonality	Clonal
Method of reprogramming	Episomal vectors
Multiline rationale	Gene corrected clones
Gene modification	YES
Type of modification	Gene correction
Associated disease	Non-syndromic retinitis pigmentosa
Gene/locus	*CLN3*/16p12.1
Method of modification	CRISPR/Cas9
Name of transgene or resistance	N/A
Inducible/constitutive system	N/A
Date archived/stock date	28/06/2016 for LEIi004-A; 21/11/2016 for LEIi004-A-1
Cell line repository/ bank	N/A
Ethical approval	Human Research Ethics Office, University of Western Australia (RA/4/1/7916)

Resource utility

Mutations in the *CLN3* gene cause juvenile neuronal ceroid lipofuscinosis (JNCL), late onset-JNCL and non-syndromic CLN3-associated retinal degeneration. Here, iPSC were generated from a patient with compound heterozygous *CLN3* mutations associated with late-onset non-syndromic retinitis pigmentosa. These lines will provide valuable insights into the pathophysiological mechanisms of *CLN3* disease.

* Corresponding author at: Centre for Ophthalmology and Visual Science, The University of Western Australia, Lions Eye Institute, 2 Verdun Street, Nedlands, 6009, Western Australia, Australia
E-mail address: fredchen@lei.org.au (F.K. Chen).

https://doi.org/10.1016/j.scr.2018.04.014
Received 21 March 2018; Received in revised form 17 April 2018; Accepted 26 April 2018
Available online 01 May 2018

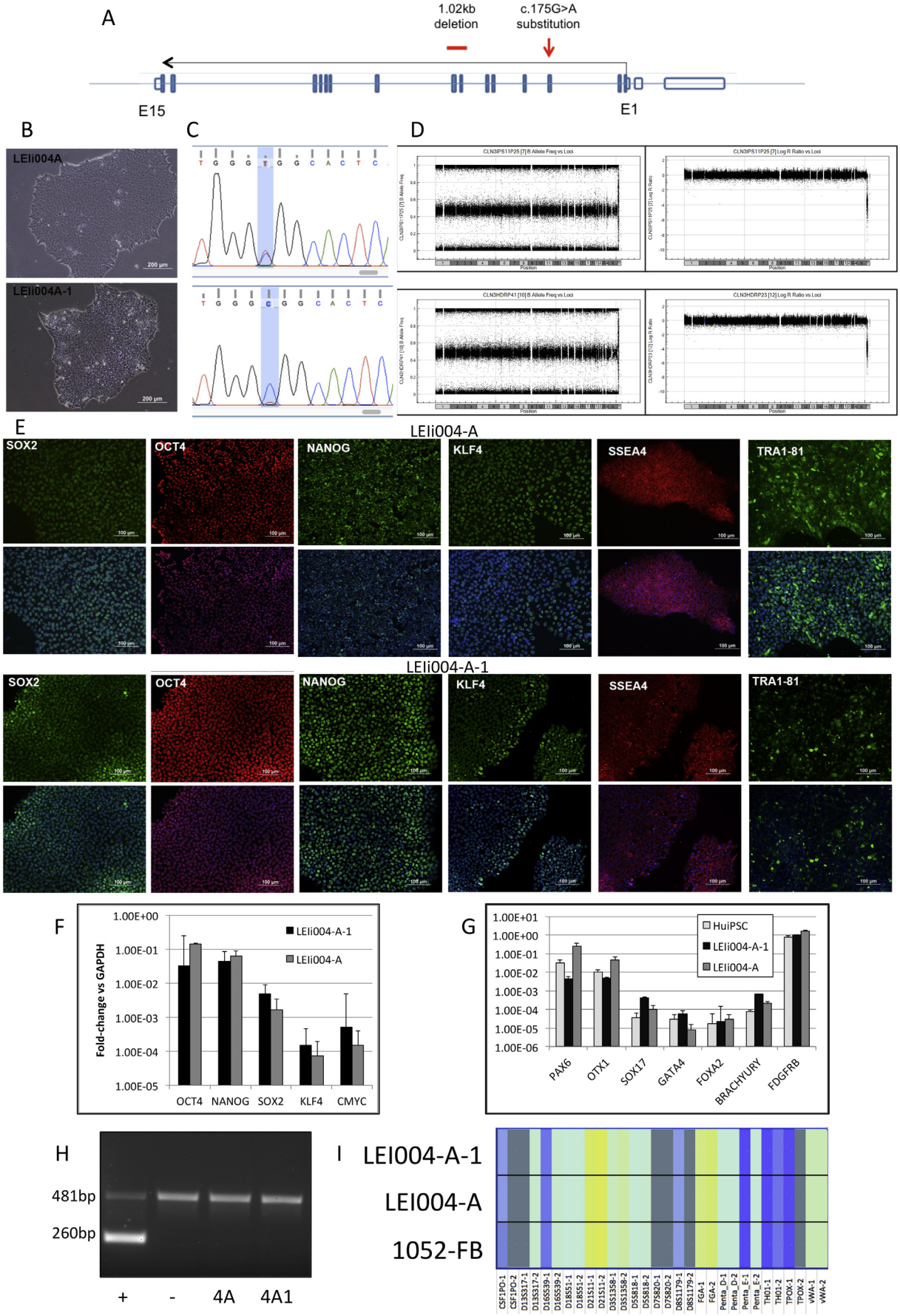

(caption on next page)

Fig. 1. A: Schematic showing the *CLN3* locus on chromosome 16 including the locations of the 1.02 kb deletion (red line) and the missense mutation (red arrow). The locations of exon 1 (E1) and exon 15 (E15) are indicated. The black arrow indicates sequence between the start and stop codons. B-D: Comparison of LEIi004-A (upper panels) and LEIi004-A-1 (lower panels). Both lines displayed morphologies consistent with pluripotent stem cell cultures (B). Sequencing of the *CLN3* gene at exon 3 demonstrated the presence of the c.175G > A mutation in LEIi004-A, but not in the gene corrected control line, LEIi004-A-1 (C). QuantiSNP analysis demonstrated a normal, 46, XX karyotype in both LEIi004-A and LEIi004-A-1 (D). E: Immunocytochemistry demonstrated the expression of pluripotency markers (SOX2, OCT4, NANOG, KLF4, SSEA4, TRA-1-81) in LEIi004-A and LEIi004-A-1. Scale bars indicate 100μm F: Quantitative RT-PCR demonstrated LEIi004-A-1 (black bars) and LEIi004-A (grey bars) expressed similar levels of the pluripotency markers OCT4, NANOG, SOX2, KLF4 and C-MYC. G: Embryoid bodies cultured from LEIi004-A and LEIi004-A-1 expressed similar levels of ectodermal (*PAX6, OTX1*), mesodermal (*SOX17, GATA4, FOXA2*) and endodermal (*BRACHYURY, FDGFRB*) genes as those cultured from a commercial iPSC line (HuiPSC). H: PCR screening demonstrated both LEIi004-A (4A) and LEIi004-A-1 (4A1) were negative for mycoplasma. Positive (+) and negative (-) controls yielded bands of the expected sizes. I: Microsatellite analysis of LEIi004-A, LEIi004-A-1 and the parental fibroblast line (1052-FB) demonstrated identity at 15 loci, indicating all three lines are derived from the same individual.

Resource details

Mutations in the *CLN3* gene cause juvenile neuronal ceroid lipofuscinosis (JNCL), an early-onset, recessive neurodegenerative disease with a prevalence of 1 in 25,000 births (Ouseph et al., 2016). Eighty percent of cases of CLN3 disease are associated with a 1.02 kb deletion that includes exons 7 and 8. However, a wide spectrum of point mutations in the *CLN3* gene have also been identified, leading to the recognition of at least two other clinical presentations of CLN3 disease, protracted JNCL (early-onset retinal degeneration with late-onset neurodegeneration) (Lauronen et al., 1999) and non-syndromic CLN3-associated retinal degeneration (Leber congenital amaurosis, early- to late-onset rod cone dystrophy, without neurodegeneration) (Ku et al., 2017; Wang et al., 2014). The clinical observation of three distinct phenotypes of CLN3 disease raises the intriguing question of why certain *CLN3* mutations spare brain, but not retinal degeneration. To provide material for investigating the pathophysiological mechanisms of CLN3 disease, we have generated human iPSCs from a 52-year old female patient diagnosed with late-onset non-syndromic CLN3-associated retinitis pigmentosa due to compound heterozygous mutations in *CLN3* (NM_000086.2), including the common 1.02 kb deletion variant and a novel variant (c.175G > A (p.Ala59Thr), rs765893479) in exon 3 (Fig. 1A, Table 1). Segregation analysis demonstrated both mutations were in separate alleles (Supp. 1).

Dermal fibroblasts were cultured from a patient skin biopsy sample. Reprogramming was performed on patient fibroblasts using non-viral and non-integrating episomal plasmids expressing *OCT4*, *SOX2*, *KLF4*, *L-MYC*, *LIN28*, *p53*shRNA, and the miR-302/367 cluster. A clonal iPSC cell line (LEIi004-A) was established and further characterized for pluripotency (Fig. 1, Table 2). To provide a coisogenic control line, the c.175G > A mutation was corrected in LEIi004-A using the CRISPR/Cas9 system. A clonal iPSC line (LEIi004-A-1) was established and further characterized for pluripotency (Fig. 1, Table 2).

The LEIi004-A and LEIi004-A-1 iPSC lines displayed morphology typical of pluripotent stem cell colonies (Fig. 1B). The c.175G > A variant was analyzed in both lines by Sanger sequencing, demonstrating the presence of the mutation in the LEIi004-A and its correction in LEIi004-A-1 (Fig. 1C). Screening for off-target modifications in LEIi004-A-1 revealed no additional mutations had been introduced by gene editing (Supp. 2). Genome-wide copy number variation profiling using the Illumina HumanCoreExome-24 Beadchip demonstrated that both clones were female and had normal diploid karyotypes (46, XX) (Fig. 1D). The expression of the pluripotency markers *OCT4*, *SOX2*, *KLF4*, *NANOG*, *c-MYC*, *SSEA4* and TRA-1-81 was demonstrated by immunostaining analyses (Fig. 1E) and quantitative real time polymerase chain reaction (qPCR) (Fig. 1F). The capacity of LEIi004-A and LEIi004-A -1 iPSC lines to differentiate into three germ layers was demonstrated by the expression of markers of ectoderm (*PAX6*, *OTX1*), mesoderm (*SOX17*, *GATA4*, *FOXA2*) and endoderm (*BRACHYURY*,

Table 1
Summary of lines.

iPSC line names	Abbreviation in figures	Gender	Age	Ethnicity	Genotype of locus	Disease
LEIi004-A	L4-A	Female	52	Caucasian	Compound heterozygous	Retinitis pigmentosa
LEIi004-A-1	L4-A-1	Female	52	Caucasian	Heterozygous	Gene corrected control

Table 2
Characterization and validation.

Classification	Test	Result	Data
Morphology	Photography	Normal	Fig. 1, Panel B
Phenotype	Immunocytochemistry	Positive for the pluripotency markers: SSEA4, TRA-1-81, OCT4, NANOG, SOX2	Fig. 1, Panel E
	Flow cytometry	N/A	
	Gene expression (qPCR)	Positive for the pluripotency markers OCT4, KLF4, SOX2, NANOG, C-MYC	Fig. 1, Panel F
Genotype	Illumina Beadchip SNP Array with CNV Analysis	LEIi004-A: 46, XX LEIi004-A-1: 46, XX Resolution: 0.5 Mb	Fig. 1, Panel D
Identity	STR analysis	Matched at 15 loci	Fig. 1, Panel I
Mutation analysis (IF APPLICABLE)	Sequencing	LEIi004-A: c.175G LEIi004-A-1: c.175A	Fig. 1, Panel C
	Southern Blot OR WGS	N/A	
Microbiology and virology	Mycoplasma	Mycoplasma testing by PCR: Negative	Fig. 1, Panel H
Differentiation potential	Embryoid body differentiation	positive for Trilineage Markers PAX6, OTX1, SOX17, GATA4, FOXA2, BRACHYURY, FDGFRB	Fig. 1, Panel G
Donor screening (OPTIONAL)	HIV 1 + 2 Hepatitis B, Hepatitis C	N/A	
Genotype additional info (OPTIONAL)	Blood group genotyping	N/A	
	HLA tissue typing	N/A	

Table 3
Reagents details.

Antibodies used for immunocytochemistry			
	Antibody	Dilution	Company Cat # and RRID
Pluripotency Markers	Mouse anti-OCT3/4	1:200	Santa Cruz Biotechnology Cat# sc-5279, RRID:AB_628051
	Rabbit anti-SOX2	1:200	Thermo Fisher Scientific Cat# 48–1400, RRID:AB_2533841
	Rabbit anti-KLF4	1:200	Abcam, Cat# ab151733, RRID: AB_2721027
	Rabbit anti-NANOG	1:100	Abcam Cat# ab21624, RRID:AB_446437
	Mouse anti-SSEA4	1:100	STEMCELL Technologies, Cat# 60062, RRID:AB_2721031
	Mouse anti-TRA-1-81-AF488	1:100	STEMCELL Technologies, Cat# 60065, RRID:AB_2721032
Secondary antibodies	Alexa Fluor 546 Goat anti-mouse	1:500	Molecular Probes Cat# A-11003, RRID:AB_141370
	Alexa Fluor 488 Goat anti-rabbit	1:500	Molecular Probes Cat# A-11008, RRID:AB_143165

Primers		
	Target	Forward/Reverse primer (5′–3′)
Episomal Plasmids	Episomal Plasmid Detection	AGGTCCCTCGAAGAGGTTCA/ TTCCAACGCGAGAAGGTGTT
Pluripotency Markers (qPCR)	SOX2	GCTACAGCATGATGCAGGACCA/ TCTGCGAGCTGGTCATGGAGTT
	OCT4	CCTGAAGCAGAAGAGGATCACC/ AAAGCGGCAGATGGTCGTTTGG
	NANOG	CTCCAACATCCTGAACCTCAGC/ CGTCACACCATTGCTATTCTTCG
	KLF4	CATCTCAAGGCACACCTGCGAA/ TCGGTCGCATTTTTGGCACTGG
House-Keeping Genes (qPCR)	GAPDH	AGAAGGCTGGGGCTCATTTG/ AGGGGCCATCCACAGTCTTC
Trilineage Markers (qPCR)	PAX6	CTGAGGAATCAGAGAAGACAGGC/ ATGGAGCCAGATGTGAAGGAGG
	OTX1	CTACCCTGACATCTTCATGCGG/ GGAGAGGACTTCTTCTTGGCTG
	SOX17	ACGCTTTCATGGTGTGGGCTAAG/ GTCAGCGCCTTCCACGACTTG
	GATA4	GCGGTGCTTCCAGCAACTCCA/ GACATCGCACTGACTGAGAACG
	FOXA2	GAACACCACTACGCCTTCAAC/ AGTGCATCACCTGTTCGTAGGC
	BRACHYURY	CCTTCAGCAAAGTCAAGCTCACC/ TGAACTGGGTCTCAGGGAAGCA
	FDGFRB	TGCAGACATCGAGTCCTCCAAC/ GCTTAGCACTGGAGACTCGTTG
Gene editing	sgRNA1	caccg CATAAGAGAAGTTGTTGCAA/ aaacTTGCAACAACTTCTCTTATGc
	sgRNA2	caccg ACGACATCCTTAGCCACAAG/ aaacCTTGTGGCTAAGGATGTCGTc
	ssODN repair template	TGAGACCTGCCCTGCTCCTTCCAGGCTGCTGGGCCTTT GCAACAACTTCTCTTATGTAGTGATGCTGAGTGCCGCC CATGACATACTTAGCCACAAGAGGACATCGGGAAACC AGAGCCATGTAAGTGACTCTCTACCACCACCACCATGG TTAGTCCCTGTGGGAAGATGAGGGGGTGG
Potential off-target site	chr7: −43,603,777	GGAGCTGGTCCATCTTGTAAA/ CTGAGACAGGATGGAATCTGTAAG
	chr10: −110,920,097	ATGCAGTTCCCACACTCAAC/ GCCACATGGTGACACGTAAT
	chr8: −60,543,401	AGCAGAACCGTGGAGATATTG/ GCTTATGCCTTGCAGATTGATT
	chr13: +40,697,429	CCGACAACCTCAACAGTCTT/ GTCATGCACATAGACTTGCTAAAC
	chr1: +59,355,714	GTGTAGAGCTTCTGGGAAAGTG/ CTCAGCGAAGTAACACCCATT
	chr18: −54,024,739	GTTTCTGCTTTCAAACAACATAGC/ TCTCTTGTCTACTGAGCCATTG
	chr1: +20,848,981	CTTAGTAAGTGACTGCCCATTTG/ TGAACTGGGTCCCTGGATA
	chrX: −67,881,060	TGAAAGAGTGCAAATGCGAAAG/ TCTCCAGACATCTCCTCAGATAC
Targeted mutation analysis/sequencing	CLN3 1.02 kb deletion	GGTTCTCGTCAGTGGGATTT/ GTCCACCCTCATCCTACTTCTA
	CLN3 c.175G > A	CGGAAGGTGATAAGGAGTGAAG/ CTGAACTTGATGCGATGGGA

FDGFRB) lineages in differentiating embryoid body cultures (Fig. 1G). Both lines were negative for mycoplasma (Fig. 1H). Analysis of 15 microsatellite markers confirmed LEIi004-A and LEIi004-A-1 were derived from the patient's fibroblasts (Fig. 1I).

Materials and methods

Ethics

Patient DNA was sourced and genetically analyzed by the Australian Inherited Retinal Disease Registry and DNA Bank, as approved by the Sir Charles Gairdner Hospital Human Research Ethics Committee (2001-053). Collection of patient samples and generation of iPSCs was approved by the University of Western Australia Human Research Ethics Committee (RA/4/1/7916). Written consent was obtained from the patient and all procedures were carried out in accordance with the requirements of the National Health & Medical Research Council of Australia and the Declaration of Helsinki.

Cell culture

Patient fibroblasts were cultured in DMEM medium supplemented with 10% fetal calf serum and antibiotic-antimycotic (ThermoFisher). Patient iPSCs were cultured in feeder-free conditions, on geltrex (ThermoFisher) coated culture plates in TeSR-E8 medium (Stem Cell Technologies). For trilineage differentiation, iPSC were cultured as embryoid bodies (EBs). IPSC were treated with Gentle Cell Dissociation buffer (Stem Cell Technologies) for 5 min at room temperature. Gentle Cell Dissociation buffer was then removed and replaced with TeSR-E8 media containing 10 μM Y27632 (Abcam) without disturbing colonies. Colonies were mechanically scraped into the media, then seeded into ultra-low attachment cell culture plates in TeSR-E8 media supplemented with 10 μM Y27632. On day 3, the media was changed to DMEM/F12 supplemented with 20% knockout serum replacement and antibiotic-antimycotic (ThermoFisher). Media was changed every second day. On day 7, EBs were plated onto geltrex coated plates and cultured for a further 7 days before harvesting RNA for qPCR analysis. Trilineage differentiation was assessed by the induction of genes for ectoderm (PAX6, OTX1) mesoderm (SOX17, GATA4, FOXA2) and endoderm (BRACHYURY, FDGFRB). Results obtained from LEIi004-A and LEIi004–A-1 were similar to those obtained with a commercial human iPSC line (Fig. 1G, HuiPSC, ThermoFisher, Cat#A18945).

Reprogramming and gene editing

Patient fibroblasts were reprogrammed using the Episomal iPSC Reprogramming Plasmid kit (SC900A-1, System Biosciences). Colonies were picked for clonal expansion on day 25. To correct the c.175G > A mutation, we employed a double nicking strategy (Ran et al., 2013). Two single guide RNA (sgRNA) sequences targeting exon 3 of *CLN3* (Table 3) were cloned into the pSpCas9(BB)-2A-Puro plasmid (PX462, Addgene) to produce two *CLN3* targeting plasmids. LEIi004-A cells were cotransfected with both targeting plasmids (2.5 μg each, 1:1 ratio) and single stranded repair template oligonucleotides (100 pmol, Table 3) using the Neon electroporation system (100 μl tip, 1100 V, 30 ms, 1 pulse, ThermoFisher). The next day, puromycin (500 ng/ml) was added to the medium. Resistant colonies were picked for clonal expansion after 7 days. Gene correction was confirmed in LEIi004-A-1 by PCR and Sanger sequencing. Potential off-target sites were predicted using online software (http://crispr.mit.edu/). Eight suspected loci were examined by Sanger sequencing.

qPCR analysis

Total mRNA was isolated using TRIZOL and cDNA was synthesized using the RT2 First Strand Kit (Qiagen). qPCR was performed using the CFX Connect Real-Time System (BioRad) and data analyzed using the ΔΔCT method. Gene expression values were normalized to GAPDH expression. Primers used are listed in Table 3.

Immunostaining analysis

Cells were fixed with 4% paraformaldehyde, washed, then permeabilized using phosphate buffered saline (PBS) with 0.1% Triton X-100 for 15 min. The cells were then incubated in 5% BSA in PBS for 1 h at room temperature. Primary antibodies were applied at 4 °C overnight. Secondary antibodies were applied for 2 h at room temperature. Nuclei were stained with DAPI. Antibodies used are listed in Table 3.

Virtual karyotyping

Virtual karyotyping was performed on all lines using the Illumina HumanCoreExome-24 Beadchip SNP array. CNV analysis was performed using GenomeStudio 2.0 (Illumina). For each line, B-allele frequencies (left panels) and logR ratios (right panels) were plotted against genomic location, demonstrating normal 46,XX karyotypes in both lines (Fig. 1D).

Microsatellite analysis

Analysis of microsatellites was performed using the Promega PowerPlex 16HS system (Promega, performed at the Australian Genome Research Facility). Patient fibroblasts (1052-FB), LEIi004-A and LEIi004-A-1 were genotyped at the loci D18S51, D21S11, TH01, D3S1358, Penta E, FGA, TPOX, D8S1179, vWA, CSF1PO, D16S539, D7S820, D13S317, D5S818 and Penta D (Fig. 1I) as well as Amelogenin (not shown). Results are shown as a heatmap, demonstrating matching genotypes at all loci examined.

Mycoplasma testing

Mycoplasma testing was performed using the Lookout Mycoplasma PCR Detection Kit (Sigma-Aldrich, Fig. 1H).

Funding

This work was funded by the National Health and Medical Research Council of Australia (grants 1142962 and 1116360), Retina Australia and generous donations from the Miocevich, Saleeba and Bone families.

Appendix A. Supplementary data

Supplementary data to this article can be found online at https://doi.org/10.1016/j.scr.2018.04.014.

References

Ku, C.A., Hull, S., Arno, G., Vincent, A., Carss, K., Kayton, R., et al., 2017. Detailed clinical phenotype and molecular genetic findings in CLN3-associated isolated retinal degeneration. JAMA Ophthalmol. 135 (7), 749–760 (Epub 2017/05/26. doi: 10.1001/jamaophthalmol.2017.1401. PubMed PMID: 28542676; PubMed Central PMCID: PMCPMC5710208).

Lauronen, L., Munroe, P.B., Jarvela, I., Autti, T., Mitchison, H.M., O'Rawe, A.M., et al., 1999. Delayed classic and protracted phenotypes of compound heterozygous juvenile neuronal ceroid lipofuscinosis. Neurology 52 (2), 360–365 (Epub 1999/02/05. PubMed PMID: 9932957).

Ouseph, M.M., Kleinman, M.E., Wang, Q.J., 2016. Vision loss in juvenile neuronal ceroid lipofuscinosis (CLN3 disease). Ann. N. Y. Acad. Sci. 1371 (1), 55–67 (Epub 2016/01/11. doi: 10.1111/nyas.12990. PubMed PMID: 26748992; PubMed Central PMCID: PMCPMC5025599).

Ran, F.A., Hsu, P.D., Wright, J., Agarwala, V., Scott, D.A., Zhang, F., 2013. Genome engineering using the CRISPR-Cas9 system. Nat. Protoc. 8 (11), 2281–2308 (Epub 2013/10/26. doi: 10.1038/nprot.2013.143. PubMed PMID: 24157548; PubMed Central PMCID: PMCPMC3969860).

Wang, F., Wang, H., Tuan, H.F., Nguyen, D.H., Sun, V., Keser, V., et al., 2014. Next generation sequencing-based molecular diagnosis of retinitis pigmentosa: identification of a novel genotype-phenotype correlation and clinical refinements. Hum. Genet. 133 (3), 331–345. Epub 2013/10/25. https://doi.org/10.1007/s00439-013-1381-5 (PubMed PMID: 24154662; PubMed Central PMCID: PMC3945441).